Ground Improvement Reinforcement Mechanisms Determined for the Mw7.8 Muisne, Ecuador, Earthquake

Miriam E. Smith, Ph.D., P.E.[1]; and Kord J. Wissmann, Ph.D., P.E., D.GE[2]

[1]Lead Engineer, Geopier Foundation Company, 130 Harbour Place Dr., Suite 280, Davidson, NC 28036. E-mail: msmith@geopier.com
[2]President, Geopier Foundation Company, 130 Harbour Place Dr., Suite 280, Davidson, NC 28036. E-mail: kwissmann@geopier.com

ABSTRACT

The 2016 Muisne, Ecuador, earthquake caused widespread soil liquefaction and structural damage as affected sites were subject to peak ground accelerations of greater than 0.4 g. Liquefaction was observed in the silty sand foundation soils adjacent to the recently constructed Briceño Bridge embankment site as evidenced by sand boils and liquefaction ejecta. However, the nearly 1 km long Briceño embankment, whose foundation materials were reinforced by relatively widely spaced rammed aggregate pier ground improvement elements, exhibited only minor damage after shaking. Post-earthquake data indicated that the ground improvement works provided densification of the SM foundation soils. This densification was not sufficient, however, to fully explain the stability of the embankment, an achievement that necessitates the presence of other stabilization mechanisms. This paper is of particular significance because it presents proposed stabilization methods that reach beyond densification in difficult to densify soils such as silty sands and sandy silts.

INTRODUCTION

News of large earthquakes in New Zealand, Nepal, China, Japan, Chile, Haiti, Indonesia, and more recently, Italy and Ecuador are certainly getting our attention. Several of these strong earthquakes have resulted in liquefaction-induced damage to infrastructure. Ground improvement methods have been used for over 70 years to densify loose sands prone to liquefaction (Mitchell et al. 1995). Rammed Aggregate Pier® (RAP) elements have been used on projects around the world for liquefaction mitigation. Their effectiveness in mitigating liquefaction in clean sandy soils has been well documented (Farrell et al. 2010; Majchrzak et al. 2010; van Ballegooy et al. 2015; Wissmann et al. 2015; Saftner et al. 2016); however, new research is demonstrating their effectiveness for liquefaction mitigation in siltier soils.

This paper presents observations from two sites in Ecuador that recently experienced shaking from the Muisne Ms7.8 earthquake. The data set collected at one of the sites provides valuable insight into the full-scale mechanisms of improvement for liquefaction-prone sites reinforced with Rammed Aggregate Pier® (RAP) elements and provides a rare and valuable data set for ground design verification.

RAP GROUND IMPROVEMENT

RAP Impact elements are constructed using displacement techniques with an excavator-mounted mobilram base machine fitted with a high frequency (30 to 40 Hz) vibratory hammer. The base machine drives a 250 to 300 mm outside diameter open-ended pipe mandrel fitted with a unique specially-designed 350 to 400 mm diameter tamper foot into the ground. The method uses hydraulic crowd pressure and vertical vibratory hammer energy to displace and densify the

liquefiable soils. Crushed gravel (typically graded at 20 to 40 mm in particle size) is fed through the mandrel from a top mounted hopper and compacted in the displaced cavities to create approximately 600 mm diameter, dense, stiff, aggregate pier elements. The construction methodology has been described in detail by Majchrzak et al. (2010) and Saftner et al. (2016).

2016 MUISNE EARTHQUAKE IN ECUADOR

On April 16, 2016, a moment magnitude Mw 7.8 earthquake, with an epicenter located about 30 km south of Muisne, struck northern Ecuador and within the first 24 hours, over 135 aftershocks were recorded. The 2016 earthquake had an economic impact estimated at 3.5% of the nation's Gross Domestic Product (Nikolaou et al. 2016). Extreme ground motions were recorded with prominent amplification and liquefaction effects at several different sites. Many structures collapsed during the seismic event, including vehicular traffic embankments that were supported on sandy soils and loose soils, which showed reliable evidence of the phenomenon of soil liquefaction.

Mejia Bridge: One such site that experienced devastating effects from the earthquake is the Mejia Bridge site, which was 78 km from the epicenter and where peak ground accelerations of 0.32 g were recorded. The subsurface conditions beneath the Mejia Bridge unsupported approach embankments generally consist of loose to medium dense silty and clayey sands with interbedded layers of medium dense gravel and sandy clay. A post-earthquake photo of the unsupported (no ground improvement) Mejia Bridge is provided in Figure 1. The sketches on Figure 1 were provided in the *GEER-ATC Earthquake Reconnaissance* report, which states that the failure surface "may be due to liquefaction-induced softening that allowed the reduced-strength soil to shear during the earthquake" (Nikolaou et al. 2016).

Figure 1. Mejía River Bridge Unsupported Approach Embankment (Nikolaou et al. 2016).

Boca de Briceño Bridge: The Boca de Briceño Bridge site is located 50 miles from the epicenter and recorded peak ground accelerations of 0.38 g during the Muisne earthquake. The soil conditions at the Briceño River bridge approach embankment are very similar to those at the Mejia Bridge embankment site and consist generally of an upper crust of silty clay underlain by loose silty sands and sandy silts, with a shallow groundwater table within 1 m below ground surface. A generalized profile of the subsurface conditions at the site is provided in Figure 2.

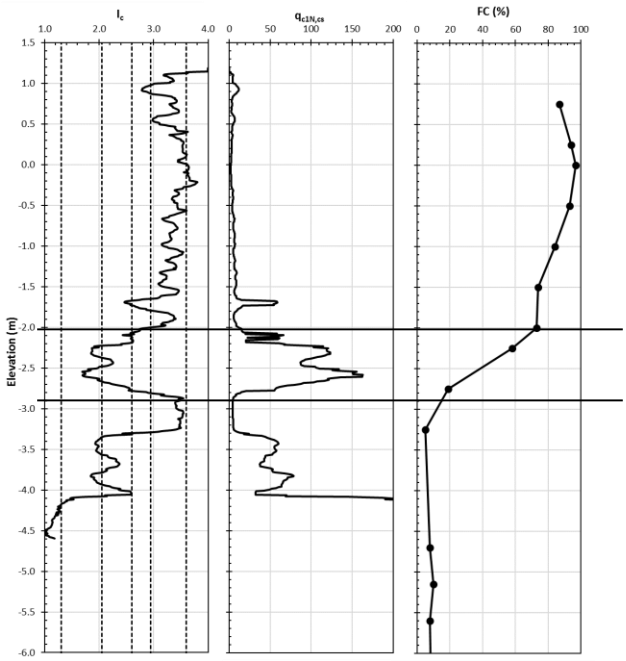

Figure 2. Generalized CPT data indicating subsurface conditions at the Briceño bridge site

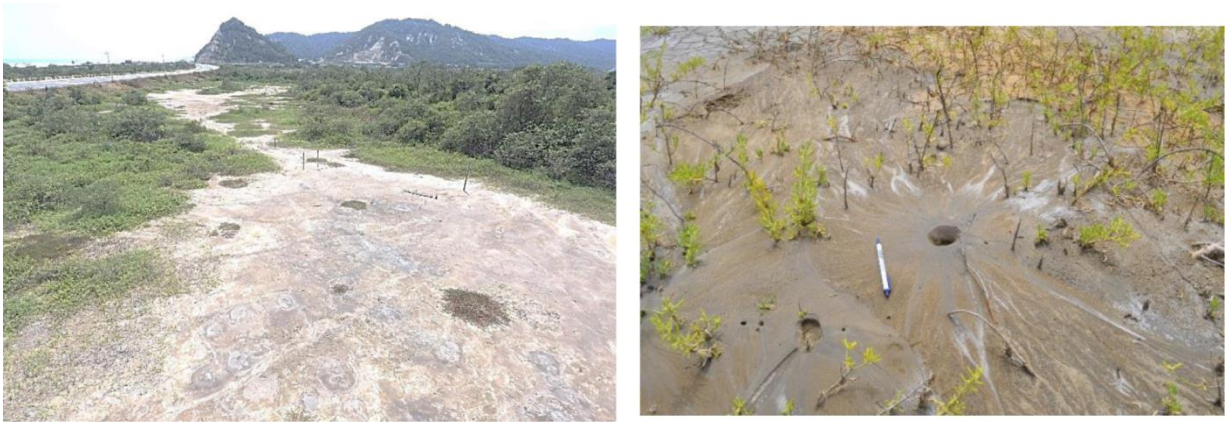

Figure 3. Sand boils indicative of liquefaction at the Boca de Briceño Bridge site (courtesy of X. Vera-Grunauer)

A new roadway at the Briceño site was constructed from 2012 to 2014. During the design phase, an approximately 1 m-thick layer of thinly interbedded sand, silty sand, and silt at a depth of about 2 to 3 m below the ground surface with pre-improvement SPT N-values of 2 to 13 and fines contents of 10% to 40% was deemed liquefiable for the design seismic event. For consistency within this article, this layer will be referred to as the "liquefiable layer." Over 6,000 RAP ground improvement elements were installed in 2012 beneath the 700 m-long Briceño bridge embankment to mitigate liquefaction potential and to increase the global stability. The 0.51 m-diameter RAPs were installed to depths of about 5 m with spacings ranging from 1.65 m at the edges up to 3 m at the center of the embankment, corresponding to area replacement ratios of 9% and 3%, respectively.

During the GEER-Earthquake Reconnaissance, evidence of liquefaction was observed within meters of the embankment in the form of sand boils and sand ejecta through cracks in the ground adjacent to the bridge abutment (Figure 3). However, the embankment exhibited minimal

damage while maintaining the serviceability of the road to the public (Figure 4).

Figure 4. Minor repairable post-earthquake damage at the RAP-supported Briceño bridge embankment (courtesy of X. Vera-Grunauer)

MECHANISMS OF LIQUEFACTION MITIGATION

Confinement and Densification: RAP Elements have been used on projects around the world for liquefaction mitigation. Their effectiveness in mitigating liquefaction in clean sandy soils has been well documented. Following the Canterbury Earthquake Sequence in New Zealand in 2010–2011, a large-scale study by the New Zealand Earthquake Commission provided a unique opportunity to investigate the efficacy of a variety of ground improvement methods for mitigating soil liquefaction and provide insight into the mechanics governing the measured response. One significant take-away from the Christchurch testing program that RAPs provide liquefaction mitigation through soil densification in soils with a soil behavior index, I_c, less than or equal to 1.8 (Wissmann et al. 2015). CPT data from 80 sites in Christchurch that supports liquefaction mitigation through densification due to RAP installation within liquefiable soils is also presented in Vautherin et al. (2017).

For the Briceño bridge site, corrected CPT tip resistance values ($q_{c1N,cs}$) within the liquefiable layer vs. the calculated Cyclic Stress Reduction (CSR) are presented in Figure 5 for each of the predominant soil classifications. The interbedded layers were separated based upon the measured soil behavior index (I_c). The free field data (triangles) plots left of the CRR line (as determined based on Idriss and Boulanger 2008) indicating liquefaction was triggered in the liquefiable layer. The calculated factors of safety against liquefaction in the SP/SM and SM/ML materials are approximately 0.27 and 0.12, respectively. These values are corroborated by the sand boils and ejecta documented outside the footprint of the Briceño bridge embankment. The values of CSR for the free-field conditions were also calculated by taking in to account the overburden stress of the embankment (i.e. confinement). These corrected values of CSR are also plotted on Figure 5 (crosses), where it can be seen that about 90% of the data points for the SM/ML and 100% of the data points for the SM/ML soils are predicted to liquefy. This suggests that confinement alone did not prevent liquefaction in the liquefiable soils.

Measured and corrected CPT tip resistance values beneath the center of the embankment within the RAP-reinforced zone are also plotted in Figure 5 (circles). The data shows an increase

in CPT tip resistance due to densification in the SP/SM soils. Due to densification alone, about 50% of the data points in the SP/SM soils move to the right of the CRR line, indicating a factor of safety against liquefaction greater than 1.0 for these points. Only minor densification is measured in the SM/ML soils, indicating that the factor of safety against liquefaction for these soils remains less than 1.0.

The data presented in Figure 5 suggests that the combined benefits of increased confinement and increased densification of the soil matrix are not sufficient to preclude liquefaction below the embankment during the design earthquake.

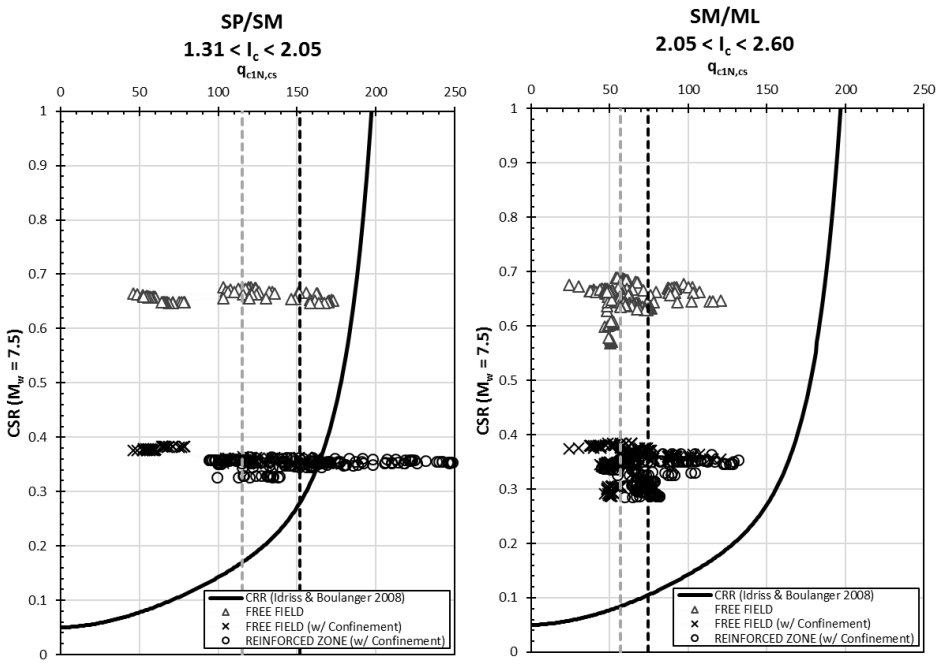

Figure 5. CPT data vs. CSR for the Briceño Bridge site

Shear Stiffening and Lateral Stress: During the Christchurch testing program, small strain crosshole shear wave velocity (Vs) testing indicated a large increase in Vs and shear modulus (G_{max}) responses for the composite RAP-reinforced ground in both clean and silty soil horizons. Large strain T-Rex testing showed that the composite reinforced ground horizons exhibited shear stiffness values greater than the unimproved soil by a factor of 3 to 5 (Wissmann et al. 2015). The results of the Christchurch test program suggest that the improvement in the liquefaction resistance of the natural soil is related to the increase in the shear stiffness response of the RAP-reinforced ground.

The stiffening effects of RAPs in liquefiable soils was studied by Green et al. (2008) and the stiffening effects of stone columns in liquefiable soils was studied by Rayamajhi et al. (2012). However, the level of shear stress reduction in the surrounding soil due to the in-situ installation of RAPs (or any other discrete column) has not been demonstrated by field data. The increase in composite shear stiffness may be explained by a variety of mechanisms. It is possible that the combination of the uncemented RAP materials combined with the vertical ramming inherent in the unique construction process of RAPs results in a well-coupled pier-soil response that transfers shear stresses effectively across the soil-pier interface. It is also possible that the liquefaction triggering is reduced by the high lateral stresses that are applied to the matrix soil during pier construction. These high lateral stresses serve to increase the mean stress conditions

of the natural soil well above the normally-consolidated stress state (Kramer 1996; Salgado et al. 1997; Handy and White 2006; Idriss and Boulanger 2008).

Figure 6 illustrates the measured V_S values at the bridge site. The composite crosshole V_S (measured across the RAP elements) values are significantly larger than those for both unimproved and improved soil because of the presence of the stiff RAP elements in the measured results. These low strain measurements are similar to those in New Zealand (Wissmann et al. 2015) and could be used to demonstrate the potential for shear stiffening at higher strain levels.

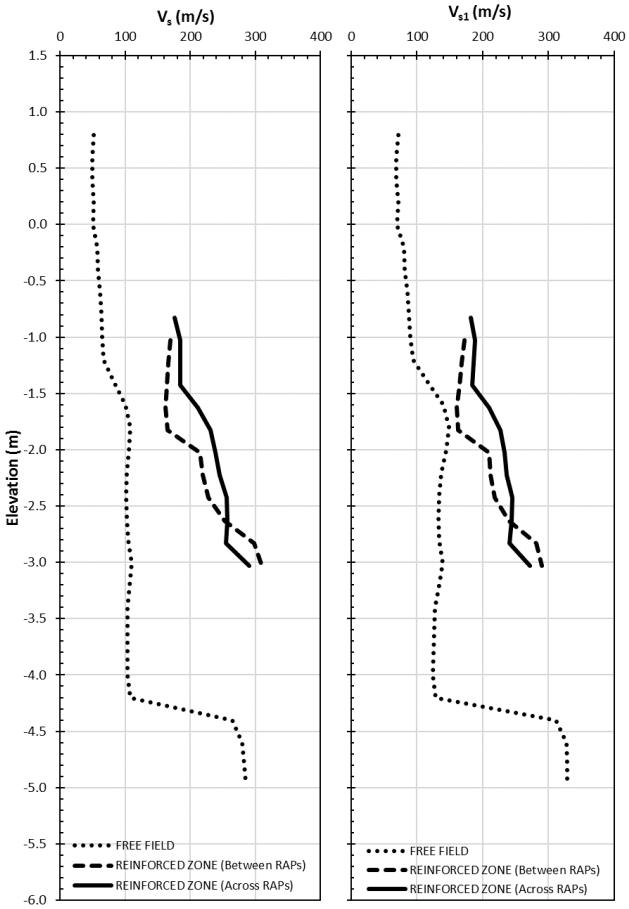

Figure 6. Post-improvement crosshole V_S profiles of the RAP improved soils

Stability: Idriss and Boulanger (2008) note that the "most severe" consequences with respect to ground deformations occur when a liquefied soil's shear strength is not sufficient to maintain stability. Idriss and Boulanger (2008) provide a CPT-based empirical formula (Equation 1) for estimating the in-situ strength of liquefied soil, $S_{residual}$:

$$\frac{S_{residual}}{\sigma_v'} = \exp\left[\frac{q_{c1}}{24.5} - \left(\frac{q_{c1}}{61.7}\right)^2 + \left(\frac{q_{c1}}{106}\right)^3 - 4.42\right] \cdot \left[1 + exp\left(\frac{q_{c1}}{11.1} - 9.82\right)\right] \leq tan\varnothing' \quad \text{Equation 1}$$

Using the CPT data from Figure 5 (plotted as triangles), the residual shear strength of the liquefiable layer in the free field was evaluated using Equation 1. A pseudo-static (k_h = 50% of the design PGA=0.40 g) limit equilibrium stability analysis of the Briceño embankment was performed using the free field residual shear strength of the liquefiable layer beneath the entire

embankment and the parameter values summarized in Table 1. This analysis yielded a factor of safety against stability of 0.97 (Figure 7). Although not performed for the Mejia bridge site, the circular failure surface indicated in this analysis correlates well with the observed failure surface beneath the Mejia bridge approach embankment (Figure 1). The CPT data from the free field corrected to for the overburden stress from the embankment (plotted as crosses in Figure 5) was also used to evaluate the residual shear strength of the liquefiable layer beneath the embankment footprint; however, this slight increase in residual shear strength only increased the factor of safety against stability to 0.98, suggesting that the Briceño embankment would have been unstable in this scenario.

Table 1. Material Property Values Used in Stability Analyses

Material	Model	Cohesion (kPa)	Friction Angle (deg)
Embankment	Mohr-Coulomb	1	34
Silty Clay / Clayey Silt	Undrained	20 kPa/m increase with depth	--
Free field residual strength (liquefiable layer)	Undrained	1	--
Measured residual strength (liquefiable layer)	Undrained	2.3	--
Dense Sand / Gravel	Mohr-Coulomb	1	37
Rammed Aggregate Pier	Mohr-Coulomb	0	45

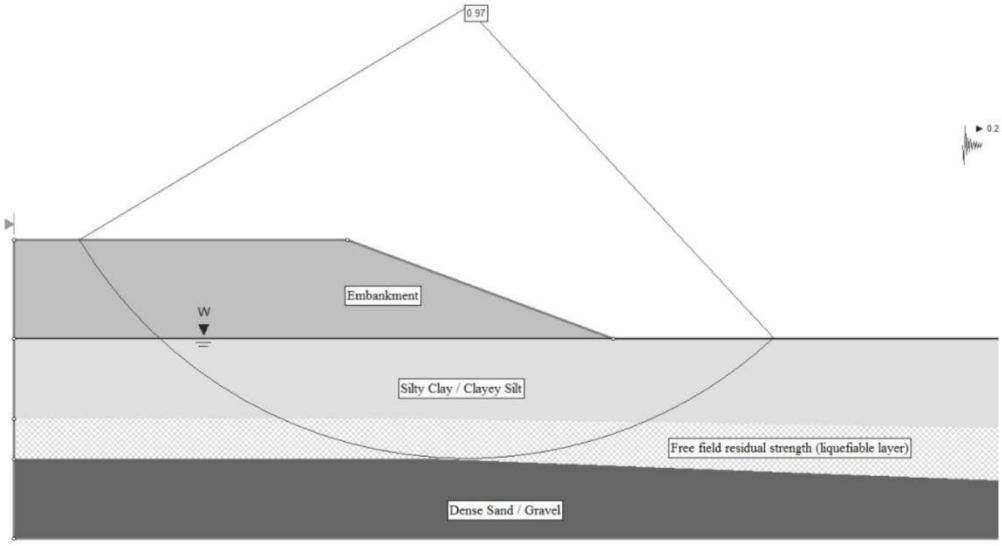

Figure 7. Pseudo-static analysis of the Briceño embankment without ground improvement

The CPT data measured beneath the embankment in the RAP-reinforced zone (plotted as circles on Figure 5) was also converted to a residual shear strength. Using this shear strength beneath the embankment footprint, factor of safety against stability increased to 1.08, which demonstrates some improvement due to densification of the matrix soil but likely not enough to prevent large deformations experienced by the embankment. The Briceño embankment experienced minimal damage following the Muisne earthquake (Figure 4) despite the sand boils

that indicate the foundation soils liquefied (Figure 3).

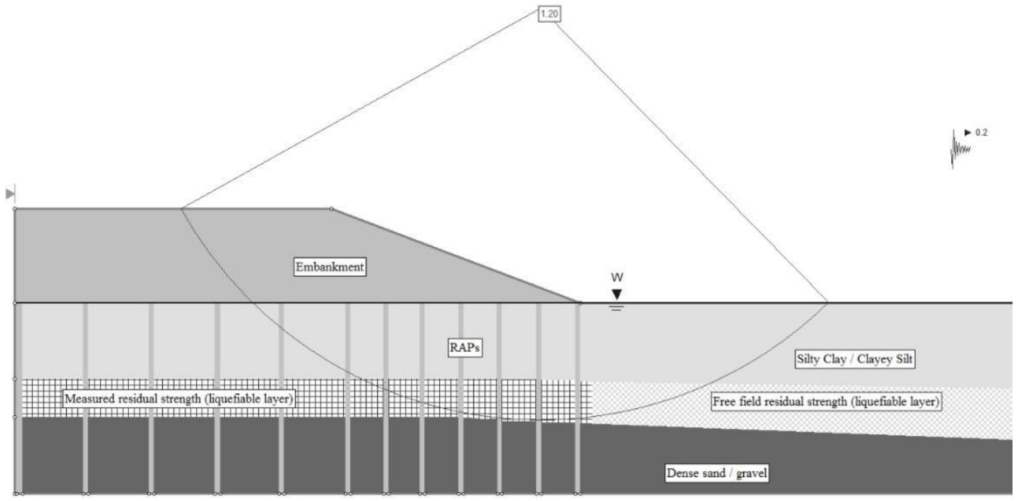

Figure 8. Pseudo-static analysis of the Briceño embankment with ground improvement

The demonstrated stability of the Briceño embankment could be explained by the composite shear wave velocity measurements (Figure 6) that suggest shear stiffening reduced shear strains to values lower than those required to trigger liquefaction. An alternate explanation is that the simple presence of the pier elements provided increased composite shear stress resistance sufficient to preclude liquefaction-induced damage. Another pseudo-static analysis was performed that included the RAPs represented by vertical panels; the results are shown in Figure 8. The width and the spacing of the panels was chosen to result in the same area replacement ratio that corresponds to the as-built conditions, as described in Navin et al. (2005). When the shear strength of the RAPs is taken into consideration, the factor of safety against stability increases from 0.97 for the unreinforced condition to 1.20. The calculated factor of safety would generally indicate that the embankment is stable with a little deformation, which was corroborated in field observations by the GEER Reconnaissance team (Nikolaou et al. 2016).

CONCLUSION

The Boca de Briceño Bridge case history summarizes the satisfactory performance of its embankment during a near-design level of PGA, with nearby evidence of liquefaction and associated damage. Despite damage to neighboring infrastructure and liquefaction triggering of the adjacent foundation soils, this embankment exhibited minimal damage while maintaining the serviceability of the road to the public (Nikolaou et al. 2016). The results of the simple pseudo-static stability analyses performed for the embankment show that while liquefaction damage was inhibited by densification resulting from pier installation, this mechanism is unlikely to fully explain the lack of appreciable embankment deformations. Embankment performance could be explained, however, by liquefaction mitigation from shear stiffening that resulted in smaller shear strains or, more simply, by simple stability analyses demonstrating the composite shear strength increase provided by the densely constructed piers.

ACKNOWLEDGEMENTS

We thank Xavier Vera-Grunauer, CEO of Geoestudios in Guayaquil, Ecuador and a member of the GEER Reconnaissance team for providing valuable observations and insight that greatly

assisted the research. We also thank Jorge Arroyo-Esqueda and Lake Carter, both with Geopier Foundation Company, for their valuable assistance in collecting and processing the field data presented herein.

REFERENCES

Farrell, T.M., Wallace, K., and Ho, J. (2010) "Liquefaction Mitigation of Three Projects in California," *Fifth International Conference on Recent Advances in Geotechnical Engineering and Soil Dynamics and Symposium in Honor of Professor I.M. Idriss*, San Diego, California, May 24–29.

Green R.A., Olgun, C.G, and Wissmann, K.J. (2008). "Shear stress redistribution as a mechanism to mitigate the risk of liquefaction." *J. Geotechnical Earthquake. Engineering & Soil Dynamics*, ASCE, IV GSP 181.

Handy, R.L, and D.J. White (2006). "Stress Zones Near Displacement Piers: Plastic and Liquefied Behavior." *ASCE. Journal of Geotechnical and Geoenvironmental Engineering*. Vol. 132. No. 1. January 2006.

Idriss, I.M. and Boulanger, R.W. (2008) *Soil Liquefaction During Earthquakes*, Monograph MNO-12, Earthquake Engineering Research Institute, Oakland, CA, 261 pp.

Kramer, S.L. (1996) Geotechnical Earthquake Engineering, Prentice Hall, New Jersey, p. 374–375.

Majchrzak, M., Farrell, T. and Metcalfe, B. (2010) "Innovative Soil Reinforcement Method to Control Static and Seismic Settlements," *Contemporary Topics in Ground Modification, Problem Soils, and Geo-support.* Geotechnical Special Publication No. 187. American Society of Civil Engineers (ASCE) Press, Reston, Va. pp. 313–320.

Mitchell, J.K., Baxter, C., and Munson, T.C. 1995. Soil Improvement for Earthquake Hazard Mitigation, *1995 ASCE National Convention*, San Diego, California, U.S., GSP 49: 836–871.

Navin, M.P., Kim, M. and Filz, G.M. (2005) "Stability of embankments founded on deep-mixing columns: three-dimensional considerations," *16th International Conference on Soil Mechanics and Geotechnical Engineering*, Osaka, Japan.

Nikolaou, S.. Vera-Grunauer, X., and Gilsanz, R. (2016). *GEER-ATC Earthquake Reconnaissance, April 16, 2016, Muisne, Ecuador*, GEER Association. Avail: https://doi.org/10.18118/G6F30N.

Rayamajhi, D., Nguyen, T.V., Ashford, S.A., Boulanger, R.W. Lu, J., Elgamal, A., and Shao, L. (2012) "Effect of Discrete Columns on Shear Stress Distribution in Liquefiable Soil, *GeoCongress 2012*, Oakland, CA.

Saftner, D.A., Zheng, J., Green, R.A., Hryciw, R., and Wissmann, K. (2016) "Rammed aggregate pier installation effect on soil properties," *Proceedings of the Institution of Civil Engineers – Ground Improvement*, Paper 1600021.

Salgado, R., Boulanger, R.W., and Mitchell, J.K. (1997) "Lateral Stress Effects on CPT Liquefaction Resistance Correlations," *Journal of Geotechnical and GeoEnvironmental Engineering*, Vol. 123, No. 8, August 1997.

van Ballegooy, S., Wentz, R., Stokoe, K., Cox, B., and Meng, F. (2015). "Dynamic Testing of Shallow Ground Improvements using a Large Mobile Shaker," *6th International Conference on Earthquake Geotechnical Engineering, 6ICEGE*, Christchurch, New Zealand, Paper No. 694.

Vautherin, E., Lambert, C., Barry-Macaulay, D. and Smith, M. (2017) "Performance of Rammed Aggregate Piers as a soil densification method in sandy and silty soils: experience from the

Christchurch rebuild," *3rd International Conference on Performance-based Design in Earthquake Geotechnical Engineering (PBD-III)*, Vancouver, BC, Canada, Paper No. 215.

Wissmann, K.J., van Ballegooy, S., Metcalfe, B., Dismuke, J., and Anderson, C. (2015). "Rammed Aggregate Pier Ground Improvement as a Liquefaction Mitigation Method in Sandy and Silty Soils," *6th International Conference on Earthquake Geotechnical Engineering , 6ICEGE*, Christchurch, New Zealand, Paper No. 216.